Anisotropic symmetric exchange as a new mechanism for multiferroicity

J. S. Feng[1,2] and H. J. Xiang[1,3,*]

[1]*Key Laboratory of Computational Physical Sciences (Ministry of Education), State Key Laboratory of Surface Physics, and Department of Physics, Fudan University, Shanghai 200433, People's Republic of China*

[2]*School of Electronic and Information Engineering, Hefei Normal University, Hefei 230601, People's Republic of China*

[3]*Collaborative Innovation Center of Advanced Microstructures, Nanjing 210093, People's Republic of China*

(Received 26 December 2015; revised manuscript received 5 April 2016; published 18 May 2016)

Discovering new magnetoelectric multiferroics is an exciting research area. Very recently, a collinear antiferromagnetic spin order was found to induce a ferroelectric polarization in a highly symmetric cubic perovskite $LaMn_3Cr_4O_{12}$. This spin-driven ferroelectricity could not be explained by any of the existing multiferroic models. Here, we put forward a new model, i.e., anisotropic symmetric exchange, to understand this phenomenon, which was confirmed by density functional calculations and tight-binding simulations. Furthermore, our perturbation analysis shows that the anisotropic symmetric exchange term can be even stronger than the conventional contributions in some 5*d* systems. Our multiferroic model can not only explain the experimental results, but also may open a new avenue for exploring exotic magnetoelectric coupling effects.

DOI: 10.1103/PhysRevB.93.174416

Multiferroics are a class of insulating materials where two (or more) primary ferroic order parameters, such as a ferroelectric polarization and long-range magnetic order, coexist [1–6]. The interest in multiferroics has been steadily increasing because of physical phenomena that result from the multiple ferroic degrees of freedom. These phenomena enable exciting innovations and new technological functionality paradigms such as novel data-storage devices for writing electrically and reading magnetically [7,8].

In particular, the so-called type-II multiferroics [9,10] are very intriguing since the ferroelectricity originates from the inversion symmetry breaking caused by the spin order, leading to a strong magnetoelectric coupling. As for the microscopic mechanisms for the spin-driven ferroelectricity, there are three well-known schemes. The first one is the spin-current mechanism [11,12]; the magnetically induced electric polarization ($\vec{P}$) is described as $\vec{P} \propto \vec{e}_{ij} \times (\vec{S}_i \times \vec{S}_j)$, where $\vec{e}_{ij}$ is a distance vector between two spins, $\vec{S}_i$ and $\vec{S}_j$. This could account for the ferroelectricity induced by a noncollinear so-called cycloidal spin order [13,14]. Another mechanism is the spin-dependent *p-d* hybridization model [15,16], which was shown to be responsible for the multiferroelectricity in $Ba_2CoGe_2O_7$ [17,18]. In the above two mechanisms, the spin-orbit coupling (SOC) is indispensable. Finally, in the exchange striction model where the SOC is not involved [19,20], the electric polarization $|\vec{P}| \propto \vec{S}_i \cdot \vec{S}_j$. Recently, these mechanisms were generalized to a unified polarization model [21,22]. To be more specific, the spin-current mechanism was extended to the general spin-current model, and the spin-dependent *p-d* hybridization model was found to be a special case of the intrasite term.

The origin of ferroelectricity in almost all type-II multiferroics can be understood with the above-mentioned models. However, an exception was found very recently. Wang *et al.* [23] discovered that a collinear antiferromagnetic order could give rise to an electric polarization in the cubic A-site ordered perovskite $LaMn_3Cr_4O_{12}$. This structure is formed when three quarters of the A site of a simple $LaCrO_3$ perovskite are substituted by Mn^{3+} ions [Fig. 1(a)]. The Cr^{3+} ion is at the center of the oxygen octahedron, while the Mn^{3+} ion is in the center of oxygen square. The neutron powder diffraction experiment showed that the Mn^{3+} and Cr^{3+} spins order in a collinear G-type AFM spin structure for both the A′-site Mn sublattice and the B-site Cr sublattice with the spin orientations along the [111] direction below 50 K. [We hereafter refer to this spin structure as AFM-I; see Fig. 1(c).] Interestingly, this AFM spin order gives rise to an electric polarization of $\sim$15 $\mu C/m^2$. It is rather surprising that the spin-driven ferroelectricity in $LaMn_3Cr_4O_{12}$ cannot be explained by the conventional mechanisms: First of all, the spin-current mechanism is not relevant since the spin order is collinear; the intrasite (including the spin-dependent *d-p* hybridization) contribution vanishes since both Mn^{3+} and Cr^{3+} ions are in the centrosymmetric positions [24]. Despite the fact that individual contribution from the exchange striction to the electric polarization is nonzero, the net contribution is zero by symmetry. So far, it remains a mystery as to what exotic mechanism is responsible for the spin-driven ferroelectricity in $LaMn_3Cr_4O_{12}$. The answer to this question will be not only relevant to the particular $LaMn_3Cr_4O_{12}$ system but may also pave a way for manipulating the magnetoelectric coupling.

In this work, we propose that there exists a previously unforeseen contribution, namely, the anisotropic symmetric exchange, to the spin-driven ferroelectricity. On the basis of density functional theory (DFT) calculation and tight-binding (TB) simulation, we demonstrate that the cubic perovskite $LaMn_3Cr_4O_{12}$ is the first system in which the anisotropic symmetric exchange is responsible for the multiferroicity.

Let us start from the discussion on the symmetry of the spin order in $LaMn_3Cr_4O_{12}$. If we only consider the Cr^{3+} (Mn^{3+}) spins, the magnetic point groups are the nonpolar $-3'$ (-3) group. Therefore, no polarization can be induced by either Cr or Mn spin ordering alone. However, when we consider Mn

*hxiang@fudan.edu.cn

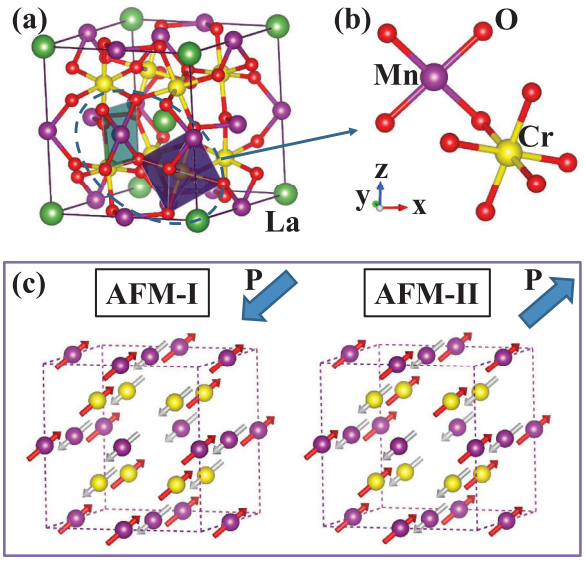

FIG. 1. (a) Crystal structure of $LaMn_3Cr_4O_{12}$ with the cubic space group $Im\bar{3}$. (b) Local structure of a nearest-neighboring Mn-Cr pair. (c) Two magnetic configurations (i.e., AFM-I and AFM-II) of $LaMn_3Cr_4O_{12}$. The corresponding ferroelectric polarizations are illustrated.

and Cr sublattices together, the magnetic point group becomes a polar group 3 with a threefold axis along the [111] direction. This suggests that the interaction between the Mn and Cr spins is the key to the ferroelectric polarization along the [111] direction. It is expected that the contribution to the electric polarization is dominated by the nearest neighboring (NN) Mn-Cr pair as shown in Fig. 1(b) since the next NN Mn-Cr distance is more than 6 Å. To the quadratic order of spins, the intersite contribution to the electric polarization induced by the spin order in the spin pair 1-2 can be written as

$$\vec{P}_{12}(\vec{S}_1,\vec{S}_2)=\sum_{\alpha\beta}\vec{P}_{12}^{\alpha\beta}S_{1\alpha}S_{2\beta}=\vec{S}_1^{\mathrm{T}}\overleftrightarrow{P}_{\mathrm{int}}\vec{S}_2, \quad (1)$$

where $\overleftrightarrow{P}_{\mathrm{int}}$ is a matrix in which each element is a vector. For convenience, we can decompose $\overleftrightarrow{P}_{\mathrm{int}}$ into three terms: $\overleftrightarrow{P}_{\mathrm{int}}=\overleftrightarrow{P}_J+\overleftrightarrow{P}_D+\overleftrightarrow{P}_\Gamma$, where $\overleftrightarrow{P}_J$, $\overleftrightarrow{P}_D$, and $\overleftrightarrow{P}_\Gamma$ are isotropic symmetric diagonal matrix, antisymmetric matrix, and anisotropic symmetric matrix. It can be easily shown that $\overleftrightarrow{P}_J$ is actually the exchange striction term, while $\overleftrightarrow{P}_D$ corresponds to the general spin-current term. Explicitly, $\overleftrightarrow{P}_\Gamma$ can be written as

$$\overleftrightarrow{P}_\Gamma=\begin{bmatrix}\vec{P}_{12}^{xx}-\frac{1}{3}(\vec{P}_{12}^{xx}+\vec{P}_{12}^{yy}+\vec{P}_{12}^{zz}) & \frac{1}{2}(\vec{P}_{12}^{xy}+\vec{P}_{12}^{yx}) & \frac{1}{2}(\vec{P}_{12}^{xz}+\vec{P}_{12}^{zx})\\ \frac{1}{2}(\vec{P}_{12}^{xy}+\vec{P}_{12}^{yx}) & \vec{P}_{12}^{yy}-\frac{1}{3}(\vec{P}_{12}^{xx}+\vec{P}_{12}^{yy}+\vec{P}_{12}^{zz}) & \frac{1}{2}(\vec{P}_{12}^{yz}+\vec{P}_{12}^{zy})\\ \frac{1}{2}(\vec{P}_{12}^{zx}+\vec{P}_{12}^{xz}) & \frac{1}{2}(\vec{P}_{12}^{zy}+\vec{P}_{12}^{yy}) & \vec{P}_{12}^{zz}-\frac{1}{3}(\vec{P}_{12}^{xx}+\vec{P}_{12}^{yy}+\vec{P}_{12}^{zz})\end{bmatrix}. \quad (2)$$

Note that $\overleftrightarrow{P}_\Gamma$ is zero if there is no SOC. In all previous studies, the anisotropic symmetric term $\overleftrightarrow{P}_\Gamma$ is disregarded. In this work, we will show that $LaMn_3Cr_4O_{12}$ is an example system where $\overleftrightarrow{P}_\Gamma$ is responsible for the spin-driven ferroelectricity.

In general, the form of the anisotropic symmetric term $\overleftrightarrow{P}_\Gamma$ can be deduced from the local symmetry of the spin pair. For example, $\overleftrightarrow{P}_\Gamma$ is zero if there is a spatial inversion symmetry in the spin pair. In the current case, the Mn-Cr spin pair has a trivial C1 point group symmetry. Thus, every element of $\overleftrightarrow{P}_\Gamma$ might be nonzero. The total electric polarization can be obtained by summing up the contributions from all the Mn-Cr pairs in $LaMn_3Cr_4O_{12}$. By doing so, we find that the electric polarization induced by the experimental magnetic structure AFM-I is $P_x=P_y=P_z=\frac{16}{3V}\sum_{\langle\alpha,\beta,\gamma\rangle}\overleftrightarrow{P}_{\Gamma,\alpha}^{\beta\gamma}$, where V is volume of the conventional cell, and $\overleftrightarrow{P}_{\Gamma,\alpha}^{\beta\gamma}$ is the anisotropic symmetry exchange term for the Mn-Cr pair shown in Fig. 1(b). Note that the summation is over all the six permutations of (x,y,z). Thus, if any of the elements $\overleftrightarrow{P}_{\Gamma,\alpha}^{\beta\gamma}$ is nonzero, the polarization is nonzero. And the polarization is along the [111] direction, in agreement with the experimental result [23].

DFT calculations with the SOC included are performed to estimate $\overleftrightarrow{P}_\Gamma$ of the Mn-Cr pair shown in Fig. 1(b). In these calculations, all the Cr^{3+} and Mn^{3+} ions are substituted by Al^{3+} ions except for the Mn-Cr pair. By computing the electric polarization of different spin configurations (in total 18) of the Mn-Cr pair, we obtain the $\overleftrightarrow{P}_\Gamma$ matrix in units of 10^{-6} eÅ:

$$\begin{bmatrix}(-0.8,-0.3,-0.5) & (-4.3,1.5,3.5) & (-2.6,1.9,1.1)\\ (-4.3,1.5,3.5) & (-2.2,4.8,5.9) & (-9.7,9.8,6.1)\\ (-2.6,1.9,1.1) & (-9.7,9.8,6.1) & (3.0,-4.5,-5.5)\end{bmatrix}. \quad (3)$$

With this $\overleftrightarrow{P}_\Gamma$ matrix, the electric polarization is computed to be $-3.2\ \mu C/m^2$ along the [111] direction. This result from the polarization model is in excellent agreement with the value ($-3.1\ \mu C/m^2$ in this study and $-3.4\ \mu C/m^2$ in Ref. [23]) from the direct DFT calculation. We consider another magnetic structure [i.e., AFM-II in Fig. 1(c)] in which all the Cr spins are reversed with respect to the AFM-I magnetic structure. Our DFT calculation and polarization model show that the AFM-II magnetic structure gives rise to an electric polarization with the same magnitude but opposite direction with respect to that in the AFM-I magnetic structure. This further validates the quadratic-spin nature of our polarization

model. This result also explains why the external electric field can control the direction of the electric polarization [23]. Note that we are considering the pure electronic contribution to the electric polarization since the atomic structure is fixed to the experimental structure. Besides the pure electronic contribution, there is a sizable ion-displacement contribution (about $-4.1\,\mu C/m^2$ [23]), resulting from the tendency to lower the anisotropic symmetric exchange interaction energy. Adding these contributions together, the magnitude of the electric polarization is now closer to the experimental value ($\sim 15\,\mu C/m^2$). Since the ion displacement induced by the spin order is too tiny to be detected experimentally, the cubic symmetry of the $LaMn_3Cr_4O_{12}$ crystal structure is apparently kept below the Neel temperature [23]. Note that the ferroelectricity induced by the collinear E-type spin order in $HoMnO_3$ was due to the isotropic symmetric exchange striction term [20], which could not explain the spin-driven ferroelectricity in $LaMn_3Cr_4O_{12}$.

The TB approach is further adopted to confirm that the anisotropic symmetric exchange is responsible for the spin-driven ferroelectricity. The $MnCrO_9$ cluster [see Fig. 1(b)] is considered in the calculation. Similar to the previous studies [16,21], our Hamiltonian includes the hopping term, the Hund term, and SOC. The single-particle wave functions $|\psi_i\rangle$ are obtained by exact numerical diagonalization, which are then used to compute the electric polarization. With the TB approach, we also find that $\overleftrightarrow{P}_\Gamma$ matrix is nonzero, resulting in an electric polarization along the [111] direction.

In the above discussion, we have unambiguously shown that the anisotropic symmetric exchange leads to the spin-order-induced electric polarization in $LaMn_3Cr_4O_{12}$. However, the total electric polarization is small ($\sim 15\,\mu C/m^2$) as compared with that in other type-II multiferroics such as $TbMnO_3$ (about $500\,\mu C/m^2$) [2]. In the following, we will discuss whether it is possible to enhance the effect of the anisotropic symmetric exchange. Since the anisotropic symmetric exchange term is an effect of SOC, we now investigate how the electric polarization depends on the magnitude of the SOC. We tune the magnitude of the SOC on Mn and Cr ions by modifying the speed of light in the DFT calculations. As shown in Fig. 2(a), the electric polarization of $LaMn_3Cr_4O_{12}$ increases rapidly with the magnitude (λ) of the SOC: When λ is doubled, the electric polarization is now 4.8 times of the original value. A similar trend is also obtained from the TB calculations [Fig. 2(b)]. This result motivates us to examine the anisotropic symmetric exchange contribution to the electric polarization in the large SOC limit.

We adopt a TB model that is closely related to that for deriving the spin-current model [11]. A key difference is that a linear M-O-M cluster is considered in the case of spin-current model, while we adopt a vertical configuration (i.e., the angle $\angle$M-O-M is 90°) in order to break the inversion symmetry of the cluster so that a nonzero anisotropic symmetric exchange could survive. Our model Hamiltonian is $H = H_0 + H_{soc} + H_U + H_t$, where H_0 is on-site energy, H_{soc} represents spin orbit coupling, H_U means Hund interaction, and H_t is hopping between the d orbitals and O $2p$ orbitals. We assume that the low-spin M ion with five d electrons is in the an oxygen octahedral ligand field (e.g., the Ir^{4+} ion in Sr_2IrO_4).

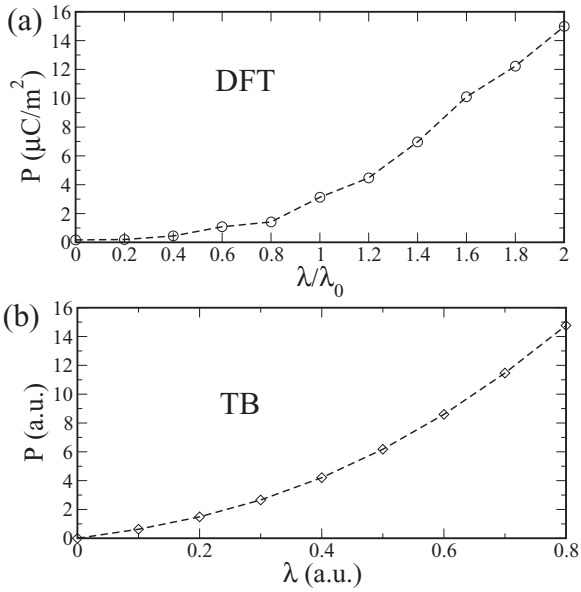

FIG. 2. (a) The dependence of the electric polarization P induced by the AFM-I state in $LaMn_3Cr_4O_{12}$ upon the magnitude (λ) of spin-orbit coupling from the DFT calculations. Panel (b) shows the corresponding result from the TB calculations.

The five d orbitals are split into threefold t_{2g} and twofold e_g manifolds. Following Katsura *et al.* [11], we will truncate the Hilbert space by considering the SOC and Hund coupling subsequently. Finally, the hopping term is treated with the second-order degenerate perturbation theory. With the particle-hole transformation [25], we now adopt the hole picture. In the strong SOC limit, the hole wave function of an M ion is the linear combination of the twofold degenerate Γ_7 states $|a\rangle, |b\rangle$. Using the two low-lying states as the basis, we can diagonalize the effective Hund term $H_U = -\mathcal{U}\sum_i \vec{m}_i \cdot \vec{S}_i$, which represents the mean-field treatment of constraining the direction of the magnetic moment $\vec{m}_i = (m_{ix}, m_{iy}, m_{iz})$. From the diagonalization, we obtain a low-lying state $|P\rangle_i$ and a high-lying state $|AP\rangle_i$, which represent the states parallel and antiparallel to the magnetic moment $\vec{m}_i$, respectively.

We are now in a stage to treat the hopping term: $H_t = H_t^{(1)} + H_t^{(2)} + \text{H.c.}$

$$H_t^{(1)} = t\sum_\sigma \left(p_{y,\sigma}^\dagger d_{xy,\sigma}^{(1)} + p_{z,\sigma}^\dagger d_{zx,\sigma}^{(1)}\right),$$
$$H_t^{(2)} = -t\sum_\sigma \left(p_{x,\sigma}^\dagger d_{xy,\sigma}^{(2)} + p_{z,\sigma}^\dagger d_{yz,\sigma}^{(2)}\right), \quad (4)$$

where $t > 0$ is the transfer integral and the superscripts (1) and (2) denote the corresponding left M ion (M_1) and up M ion (M_2) respectively. The low-energy Hibert space now contains $|P\rangle_1$, $|P\rangle_2$, and O $|p_{x,\uparrow}\rangle$, $|p_{x,\downarrow}\rangle$, $|p_{y,\uparrow}\rangle$, $|p_{y,\downarrow}\rangle$, $|p_{z,\uparrow}\rangle$, $|p_{z,\downarrow}\rangle$. Second-order degeneration perturbation theory is used to obtain the first-order hole wave functions ψ_i. The electric polarization of the system is computed by $\mathbf{P} = \sum_k \langle\psi_k|\mathbf{r}|\psi_k\rangle$, where the summation ($k = 1,2$) is over the two low-lying hole wave functions.

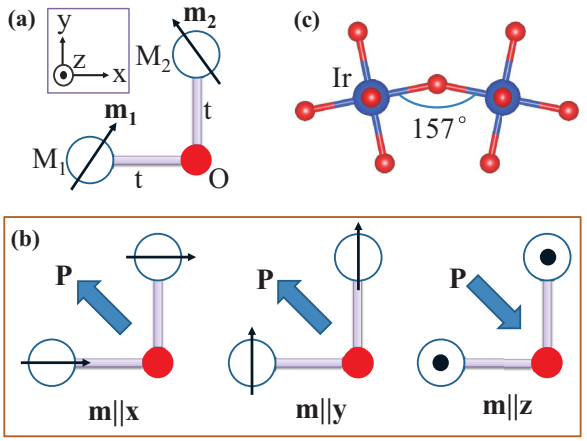

FIG. 3. (a) Schematic illustration of the three-atom cluster with $\angle M_1\text{-O-}M_2 = 90^\circ$. The directions of the magnetic moments ($\mathbf{m}_1$ and $\mathbf{m}_2$) are denoted by arrows. The hopping between the metal M t_{2g} orbitals and O $2p$ orbitals is represented as "t." (b) Predicted electric polarizations of the M_1-O-M_2 cluster induced by three different ferromagnetic configurations ($\mathbf{m}||x$, $\mathbf{m}||y$, or $\mathbf{m}||z$). (c) The local structure of the nearest-neighboring Ir-Ir pair in Sr_2IrO_4.

After a detailed derivation, we obtain the spin-order-induced polarization as

$$\begin{aligned} P_x &= -P_y = \frac{t^3}{9\Delta^3}(I_1 + I_2)(m_{1x}m_{2y} - m_{2x}m_{1y}) \\ &\quad + \frac{I_1 t^3}{9\Delta^3}(m_{1z}m_{2z} - m_{1x}m_{2x} - m_{1y}m_{2y}), \\ P_z &= \frac{I_1 t^3}{9\Delta^3}(m_{1y}m_{2z} + m_{2y}m_{1z} - m_{1x}m_{2z} - m_{2x}m_{1z}). \end{aligned} \quad (5)$$

Here, Δ is the energy difference between the $|P\rangle_i$ orbital and O $2p$ orbital, and I_1 and I_2 are the dipole matrix elements with $\langle p_x|y|d^{(1)}_{xy}\rangle = \langle p_x|y|d^{(2)}_{xy}\rangle = I_1, \langle p_y|z|d^{(1)}_{yz}\rangle = \langle p_x|z|d^{(2)}_{zx}\rangle = I_2$. From the expressions of polarization in Eq. (5), the spin-order-induced polarization has both an out-of-plane component and an in-plane component. Interestingly, the in-plane component is always along the $[1\bar{1}0]$ direction independent of the spin orientation. Since the polarization contains only second-order terms of spin directions [see Eq. (5)], the polarization can be exactly decomposed into the general spin current term, exchange striction term, and anisotropic symmetric exchange term. The anisotropic symmetric exchange $\overleftrightarrow{P}_\Gamma$ is expressed as

$$\overleftrightarrow{P}_\Gamma = \frac{I_1 t^3}{9\Delta^3}\begin{bmatrix} (-2/3,2/3,0) & (0,0,0) & (0,0,-1) \\ (0,0,0) & (-2/3,2/3,0) & (0,0,1) \\ (0,0,-1) & (0,0,1) & (4/3,-4/3,0) \end{bmatrix}. \quad (6)$$

To our surprise, we find that the anisotropic symmetric exchange term is giant, as can be seen from the fact that the polarization induced by the ferromagnetic spin configuration along the z axis is opposite to that by the in-plane ferromagnetic spin configuration [see Fig. 3(c)]. The exchange striction term is $\overrightarrow{P}_J(\overrightarrow{S}_1 \cdot \overrightarrow{S}_2)$ with $\overrightarrow{P}_J = \frac{I_1 t^3}{9\Delta^3}(-1/3,1/3,0)$. It can be seen that $\overleftrightarrow{P}_\Gamma$ is even larger than the exchange striction term and general spin current term (see Supplemental Material [26]). Our main results from the perturbation theory are further confirmed by our exact diagonalization study.

Thus, with a TB approach, we find a large anisotropic symmetry exchange term in a nonlinear M-O-M model. In the following, we will argue that this phenomenon may take place in some realistic materials. Recently, the layered perovskite Sr_2IrO_4 has attracted much interest due to the presence of the $J_{\text{eff}} = 1/2$ spin-orbital Mott insulating state. Sr_2IrO_4 has a tetragonal K_2NiF_4-like crystal structure as illustrated in Fig. S1 of the Supplementary Material. The IrO_6 octahedra are rotated and tilted so that the Ir-O-Ir angle is about 157°. Therefore, the anisotropic symmetry exchange should be nonzero since the Ir-O-Ir angle is not 180°. Our DFT calculations provide evidence that the anisotropic symmetry exchange in Sr_2IrO_4 is indeed strong. In these calculations, we replace all the Ir^{4+} ions by Si^{4+} ions except for a NN Ir-Ir pair. Three AFM states of the Ir-Ir spin pairs are considered: The spins are along the x, y, or z axis. We find the difference in the electric polarization between AFM-x state and AFM-z state is larger than that between AFM-x and AFM-y state. And this difference (about 0.009 eÅ) is almost three orders of magnitude larger than the corresponding value in $LaMn_3Cr_4O_{12}$. Since a giant magnetoelectric effect was discovered experimentally in Sr_2IrO_4 [35], we speculate that the anisotropic symmetry exchange may play an important role in the exotic magnetoelectric coupling. Note that the isotropic symmetry exchange could give rise to a ferroelectric polarization as large as several $\mu C/cm^2$ [20,36], which is large enough for realistic applications. It is expected that the anisotropic symmetric exchange might also give rise to a large ferroelectric polarization. We should note that the magnetoelectric coupling in magnetic multiferroics is intrinsically strong since the ferroelectric polarization is induced directly by a spin order.

In summary, on the basis of first-principles theory and the TB approach, we demonstrate that the spin-driven ferroelectricity in the cubic perovskite $LaMn_3Cr_4O_{12}$ is due to a new mechanism, namely, the anisotropic symmetric exchange, which has not been taken into account in previous multiferroic models. Although usually the anisotropic symmetric exchange is weak, it becomes even stronger than the symmetric exchange striction term and spin-current term for a nonlinear M-O-M cluster in the large SOC limit. This may account for the giant magnetoelectric effect experimentally observed in iridates.

Work was supported by NSFC (11374056), the Special Funds for Major State Basic Research (2012CB921400, 2015CB921700), Program for Professor of Special Appointment (Eastern Scholar), Qing Nian Bo Jian Program, and Fok Ying Tung Education Foundation. H.X. thanks Dr. Yisheng Cai, Dr. Young Sun, and Dr. Youwen Long for useful discussions.

[1] J. Wang, J. B. Neaton, H. Zheng, V. Nagarajan, S. B. Ogale, B. Liu, D. Viehland, V. Vaithyanathan, D. G. Schlom, U. V. Waghmare, N. A. Spaldin, K. M. Rabe, M. Wuttig, and R. Ramesh, Science **299**, 1719 (2003).

[2] T. Kimura, T. Goto, H. Shintani, K. Ishizaka, T. Arima, B. Liu, and Y. Tokura, Nature (London) **426**, 55 (2003).

[3] S.-W. Cheong and M. Mostovoy, Nat. Mater. **6**, 13 (2007).

[4] K. Wang, J.-M. Liu, and Z. Ren, Adv. Phys. **58**, 321 (2009).

[5] T. Birol, N. A. Benedek, H. Das, A. L. Wysocki, A. T. Mulder, B. M. Abbett, E. H. Smith, S. Ghosh, and C. J. Fennie, Curr. Opin. Solid. St. M **16**, 227 (2012).

[6] J. Young, A. Stroppa, S. Picozzi, and J. M. Rondinelli, J. Phys.: Condens. Mat. **27**, 283202 (2015).

[7] N. A. Spaldin and M. Fiebig, Science **309**, 391 (2005).

[8] J. F. Scott, Nature (London) **6**, 256 (2007).

[9] D. Khomskii, Physics **2**, 256 (2009).

[10] Y. Tokura and S. Seki, Adv. Mater. **22**, 1554 (2007).

[11] H. Katsura, N. Nagaosa, and A. V. Balatsky, Phys. Rev. Lett. **95**, 057205 (2005).

[12] I. A. Sergienko and E. Dagotto, Phys. Rev. B **73**, 094434 (2006).

[13] H. J. Xiang, S.-H. Wei, M.-H. Whangbo, and J. L. F. Da Silva, Phys. Rev. Lett. **101**, 037209 (2008).

[14] A. Malashevich and D. Vanderbilt, Phys. Rev. Lett. **101**, 037210 (2008).

[15] T. Arima, J. Phys. Soc. Jpn **76**, 073702 (2007).

[16] C. Jia, S. Onoda, N. Nagaosa, and J. H. Han, Phys. Rev. B **74**, 224444 (2006).

[17] H. Murakawa, Y. Onose, S. Miyahara, N. Furukawa, and Y. Tokura, Phys. Rev. Lett. **105**, 137202 (2010).

[18] K. Yamauchi, P. Barone, and S. Picozzi, Phys. Rev. B **84**, 165137 (2011).

[19] I. A. Sergienko, C. Şen, and E. Dagotto, Phys. Rev. Lett. **97**, 227204 (2006).

[20] S. Picozzi, K. Yamauchi, B. Sanyal, I. A. Sergienko, and E. Dagotto, Phys. Rev. Lett. **99**, 227201 (2007).

[21] H. J. Xiang, E. J. Kan, Y. Zhang, M.-H. Whangbo, and X. G. Gong, Phys. Rev. Lett. **107**, 157202 (2011).

[22] H. J. Xiang, P. S. Wang, M.-H. Whangbo, and X. G. Gong, Phys. Rev. B **88**, 054404 (2013).

[23] X. Wang, Y. Chai, L. Zhou, H. Cao, C.-D. Cruz, J. Yang, J. Dai, Y. Yin, Z. Yuan, S. Zhang, R. Yu, M. Azuma, Y. Shimakawa, H. Zhang, S. Dong, Y. Sun, C. Jin, and Y. Long, Phys. Rev. Lett. **115**, 087601 (2015).

[24] J. H. Yang, Z. L. Li, X. Z. Lu, M.-H. Whangbo, S.-H. Wei, X. G. Gong, and H. J. Xiang, Phys. Rev. Lett. **109**, 107203 (2012).

[25] G. S. Tian, Phys. Lett. A **228**, 383 (1997).

[26] See Supplemental Materials http://link.aps.org/supplemental/10.1103/PhysRevB.93.174416 for details, which includes Refs. [27–34], for computation details on the density functional theory (DFT) calculations, a detailed analytical derivation of the tight-binding (TB) treatment of the nonlinear M-O-M cluster, and the crystal structure of Sr_2IrO_4.

[27] J. P. Perdew, K. Burke, and M. Ernzerhof, Phys. Rev. Lett. **77**, 3865 (1996).

[28] A. I. Liechtenstein, V. I. Anisimov, and J. Zaanen, Phys. Rev. B **52**, R5467 (1995).

[29] P. E. Blöchl, Phys. Rev. B **50**, 17953 (1994).

[30] G. Kresse and D. Joubert, Phys. Rev. B **59**, 1758 (1999).

[31] G. Kresse and J. Furthmller, Comp. Mater. Sci. **6**, 15 (1996).

[32] G. Kresse and J. Furthmüller, Phys. Rev. B **54**, 11169 (1996).

[33] R. D. King-Smith and D. Vanderbilt, Phys. Rev. B **47**, 1651 (1993).

[34] R. Resta, Rev. Mod. Phys. **66**, 899 (1994).

[35] S. Chikara, O. Korneta, W. P. Crummett, L. E. DeLong, P. Schlottmann, and G. Cao, Phys. Rev. B **80**, 140407 (2009).

[36] T. Aoyama, K. Yamauchi, A. Iyama, S. Picozzi, K. Shimizu, and T. Kimura, Nat. Commun. **5**, 4927 (2014).